The enhanced MR performance of dimorphic MR suspensions containing either magnetic rods or their non-magnetic analogues

Tomas Plachy, Martin Cvek, Zuzana Kozakova, Michal Sedlacik, Robert Moucka

Centre of Polymer Systems, University Institute, Tomas Bata University in Zlin, Trida Tomase Bati 5678, 760 01 Zlin, Czech Republic
Email: plachy@cps.utb.cz

Abstract

A co-precipitation method was used to prepare non-magnetic rod-like ferrous oxalate dihydrate (Fe_2CO_4•$2H_2O$) particles that were further turned into iron oxide (Fe_3O_4) magnetic rod-like particles. A simple precursor-assisted thermal decomposition technique enabled the preservation of the morphology and size of the precursor ferrous oxalate dihydrate particles, thus allowing their magnetic analogues to be obtained. Both types of rod-like particles were used as an additive together with spherical carbonyl iron particles in novel dimorphic magnetorheological suspensions. Controlled shear rate mode experiments were performed using a rotational rheometer with a source of an external magnetic field in order to investigate their magnetorheological behavior. Moreover, the properties of the novel prepared dimorphic magnetorheological suspensions were compared with conventional magnetorheological suspensions based on spherical carbonyl iron microparticles. It was found that the dimorphic magnetorheological suspensions exhibit enhanced magnetorheological performance as well as enhanced sedimentation stability in comparison with the magnetorheological suspension based on pure carbonyl iron. The dimorphic suspensions containing magnetic rod-like additives further exhibited significant magnetorheological hardening at low shear rates. The properties of carbonyl iron-based suspensions can be thus optimized by using various additive substances.

Introduction

Magnetorheological (MR) suspensions are systems, the rheological parameters of which can be controlled via an external magnetic field. They are generally composed of a non-magnetic liquid medium in which magnetically-polarizable particles are dispersed. Upon the application of an external magnetic field, the dispersed magnetic particles start to create organized column-like structures leading to an abrupt increase in the rheological parameters (yield stress, viscosity, viscoelastic moduli) of the system due to the magnetic dipole-dipole attraction of the particles.

This behavior is called the MR effect. Magnetorheological suspensions then exhibit yield stress, τ_y, which is a function of the intensity of an applied magnetic field [1-3], H_0, the volume fraction of the particles, ϕ, their morphology [4, 5] and their magnetic properties (saturation magnetization, M_S, magnetic permeability, μ, and magnetic susceptibility, χ) [6, 7], and are of great interest in many industrial areas. They can be utilized, e.g., in the automotive industry as a medium in dampers [8, 9] (and generally in many other damping systems), clutches [10] or brakes [11]. They are further used in civil engineering to counteract vibrations in cable-stayed bridges and high-rises caused by seismic activity [8] or sudden wind gusts [12, 13].

Magnetorheological suspensions commonly consist of spherical carbonyl iron (CI) particles dispersed in a liquid medium [14]. The main criteria of MR suspensions determining their applicability are the high intensity of the MR effect, high sedimentation stability [15] from a long-term point of view, and easy redispersibility. Recently, so-called dimorphic MR (DMR) suspensions, which are composed of two different types of magnetic particles, have been introduced [16-20]. This unusual composition, when the various particles are used to form solid particle fractions in suspension, can lead to a higher τ_y of such MR systems and can pronounce their sedimentation stability [19-21] as well as their redispersibility. Not only have variously-shaped magnetic particles been involved in the creation of DMR suspensions, but also various non-magnetic materials have been recently used as an additive in MR suspensions [22, 23]. Additives such as clay materials [21], carbon fatty acids [24, 25], or silica [24] can be used in MR suspensions to suppress the sedimentation or increase MR effects. It has been shown that the addition of a small amount of non-magnetic or purely magnetic rod-like [19] or plate-like [22] particles can lead to a significant increase in the shear stress values of MR suspensions. Bombard et al. [16] employed magnetic and non-magnetic nanorods into spherical iron particles, which increased the MR effects of DMR suspensions when compared to MR suspensions based on pure spherical iron particles. Also, the addition of non-magnetic spherical particles into MR suspensions led to a significant increase in MR effects due to increased viscous dissipation and rotary diffusivity [23].

In order to compare the roles of the magnetic and non-magnetic micro-sized rod-like filler in the MR suspensions based on CI particles, magnetic field-responsive DMR suspensions were prepared. The two step synthesis enables the obtainment of magnetic and non-magnetic rod-like particles of the same shape and size, which were used together with CI particles for novel DMR suspensions. In addition, the prepared rod-like particles were of a length in a range between 10–30 μm, which has not yet been introduced in magnetorheology (commonly,

significantly smaller rod-like particles are used). The MR behavior of the prepared DMR suspensions as well as MR suspensions consisting only of CI of the same weight fraction were investigated in steady-shear mode.

Experimental part

A synthesis of the particles

The particles were prepared via a two-step synthesis similar to a procedure presented by Kozakova et al. [26]:

(i) The iron(II) oxalate dihydrate ($Fe_2CO_4 \bullet 2H_2O$) non-magnetic rods (the precursor) were prepared via a co-precipitation method using a microwave oven. Twenty mmoL of iron(II) suplhate heptahydrate (Sigma Aldrich) and oxalic acid dihydrate (Lach-Ner; Czech Republic) were separately dissolved in a 28 mL mixture of ethyleneglycol (Penta; Czech Republic) and demineralized water 3:1 (v/v). The oxalic acid solution was then slowly added into the iron sulphate solution under stirring using a magnetic stirrer. The mixture was subsequently placed into a cavity of a pressurized microwave reactor, CEM Mars 5 (USA), and treated for 30 minutes at 100°C at an elevated pressure. Then, the product was filtered and rinsed off with an excess of water in order to remove the impurities and mainly the ethylenglycol from a filter cake. Finally, the sample was dried at 70°C under 200 mbar in a vacuum oven. These non-magnetic particles are further labelled as Sample 1.
(ii) Fe_3O_4 magnetic rods were obtained from Sample 1 using a thermal decomposition process. Firstly, 250 mg of Sample 1 was put into a sealing ampule of a total volume of 50 mL. The ampules were sealed in order to avoid the entrance of the additional air containing oxygen. Then, the ampules were put into a furnace pre-heated to 400°C and the particles were treated at 400°C for 25 min. The particles were subsequently removed from the furnace and left to cool down to a room temperature. After cooling, the ampules were carefully opened and the magnetic particles were collected. Such particles are further labelled as Sample 2.

Preparation of the MR and DMR suspensions

The reference MR suspension was prepared by suspending the CI (ES grade, BASF, Germany) in silicone oil (Lukosiol M200, Chemical Works Kolin, Czech Republic, viscosity η_c = 194 mPa s) at a weight ratio of 60:40. The DMR suspensions were prepared by replacing some portion of the CI with the same weight percentage of either $Fe_2CO_4 \bullet 2H_2O$ (Sample 1) or Fe_3O_4 (Sample 2). The compositions of the prepared MR and DMR suspensions are listed in

table 1. The prepared MR and DMR suspensions were thoroughly mixed in a beaker with a glass stick for 5 minutes before each measurement.

Table 1. – Compositions of the prepared MR and DMR suspensions

	Carbonyl iron (wt%)	$Fe_2CO_4 \bullet 2H_2O$ (wt%)	Fe_3O_4 (wt%)	Silicone oil (wt%)
MR	60	0	0	40
DMR1–2.5	57.5	2.5	0	40
DMR1–5	55	5	0	40
DMR2–2.5	57.5	0	2.5	40
DMR2–5	55	0	5	40

Characterization of the particles, MR suspensions, and sedimentation stability

X-ray diffraction (XRD) patterns were obtained using an X-ray diffractometer Miniflex 600 (Rigaku, Japan) in order to confirm the successful preparation of the precursor and its further transition into magnetic Fe_3O_4 particles. The XRD patterns were collected in an angle range of 10–95° 2θ with Co Kα1 radiation. The results were compared with a database. The morphology and the dimensions of the particles were observed using scanning electron microscopy (SEM; Phenom Pro, The Netherlands and Nova NanoSEM 450, FEI, USA). Magnetization curves of the particles were measured by a vibrational sample magnetometer (VSM; Model 7404, Lake Shore, USA) in the magnetic field range of ±760 kA m^{-1}. Controlled shear rate rheological experiments in the absence and in the presence of an external magnetic field in the direction perpendicular to the shearing with an intensity of 87–438 kA m^{-1} were performed using a rotational rheometer (MCR 502 Anton Paar, Austria) with an external magnetic cell using parallel-plate geometry with a diameter of 20 mm at 20 °C and a gap fixed at 500 μm. The experiments were performed in the shear rate range of 0.1–300 s^{-1} and before each measurement in the presence of the external magnetic field. The magnetic field was applied 2 minutes before the beginning of the shearing in order to provide enough time for particles to create stable internal structures.

The sedimentation stabilities of the prepared MR, DMR1–5 and DMR2–5 suspensions were investigated at 20 °C using the visual method. The prepared suspensions were diluted to a total particle concentration of 10 wt% and thoroughly manually stirred for 5 minutes and then mixed using an ultrasonic bath (UZ Sonopuls HD 2070 Kit, Germany) for approximately 2 minutes. A dilution of the prepared suspensions was performed to further the feasibility of the sedimentation measurement. The well-mixed suspensions were subsequently transferred into

cylindrical tubes. The sedimentation ratio was calculated as the ratio of the height of the volume containing the particles and the height of the total volume of the suspensions.

Results

Particle characterization

The XRD pattern of the prepared precursor (figure 1) has confirmed the successful preparation of $FeC_2O_4 \bullet 2H_2O$, since all characteristic peaks can be read. The small peak at $2\theta=33°$ can be assigned to the low contamination of the product by the unconsumed reactants. All the XRD pattern peaks of the prepared Sample 2 can be attributed to Fe_3O_4 without other crystalline impurities.

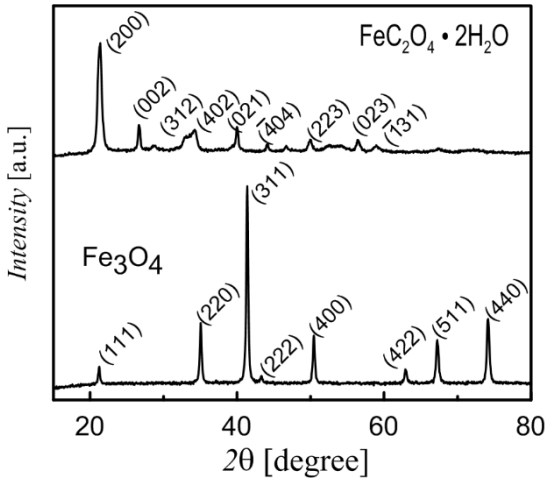

Figure 1. XRD patterns of the prepared Sample 1 particles (top line) and Sample 2 particles (bottom line).

The commercial CI particles possess a regular spherical shape (figure 2(a)) with a mean diameter d_{50} ranging between 3.4–4.5 μm (values guaranteed by the supplier) and relatively high polydispersity. Figure 2(b) confirms the rod-like shape of Sample 1. The rod-like particles are around 10–30 μm long and possess a high aspect ratio. After the thermal treatment, which caused the development of the magnetic Fe_3O_4 particles, the shape, size and morphology of the particles were preserved (figure 2(b,c)). In this kind of synthesis, the shrinkage process becomes significant only in the case of higher temperatures; therefore, in this study the particle size was preserved [27]. Nevertheless, due to the thermal decomposition process and the further sintering of the prepared Fe_3O_4 particles together, the internal structure of Sample 2 when compared with Sample 1 is changed. Sample 2 is obviously composed of small Fe_3O_4 particles, leading to the

higher porosity of the system with a significant free space between the particles (figure 2(d,e)) [27].

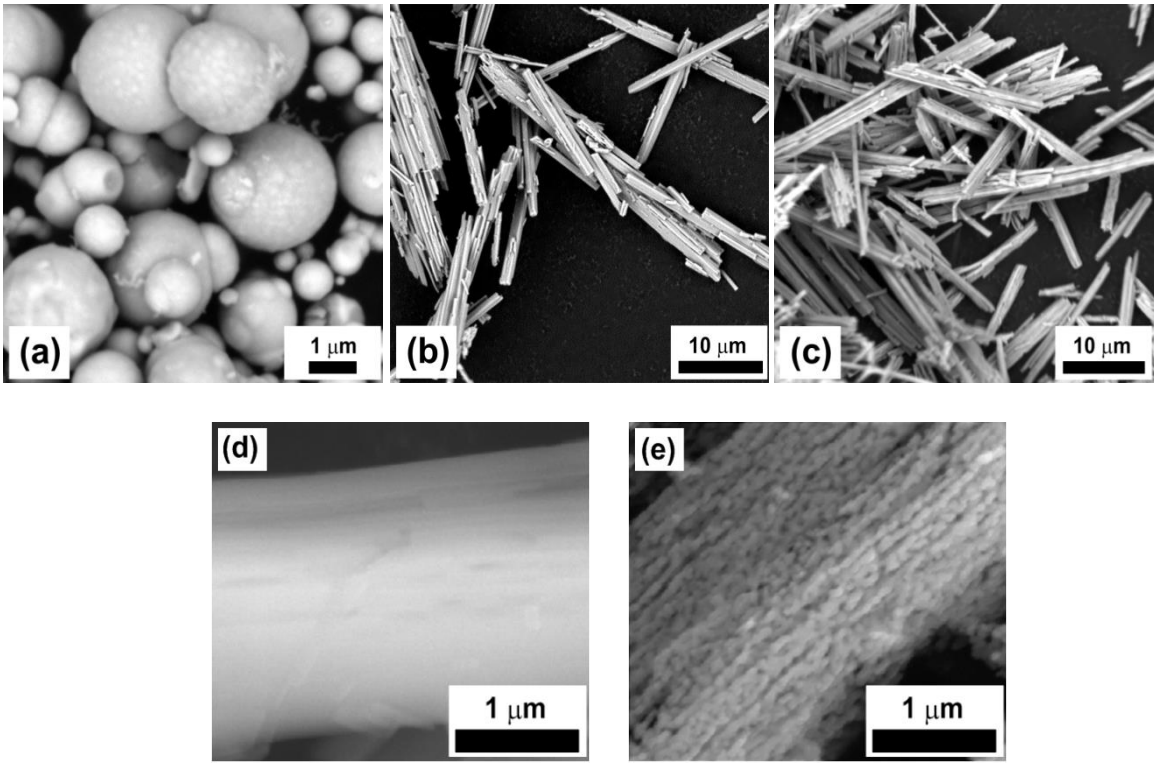

Figure 2. SEM images of (a) CI particles; (b), (d) Sample 1 particles; and (c), (e) Sample 2 particles.

The magnetization curves of the CI and Sample 2 are depicted in figure 3. Clear saturation magnetization, M_S, was not achieved since the curves did not exhibit a plateau in an investigated region; therefore, the maximum magnetization values, M_{max}, at the highest H_0 used in the MR measurements are found in figure 3. It can be seen that the highest M_{max} was observed for bare CI particles (=173.9 emu g^{-1}). The Sample 2 particles exhibited M_S = 56.1 emu g^{-1}, which is significantly lower than for the CI. This is due to the chemical composition of Sample 2, which is composed of ferrite oxides possessing lower magnetization than pure CI. The hysteresis (remanent magnetization) of the Sample 2 particles was sufficiently low, enabling a quick demagnetization process. Sample 1 is a non-magnetic material; therefore, its magnetization was not investigated and is supposed to be ~ 0 emu g^{-1}.

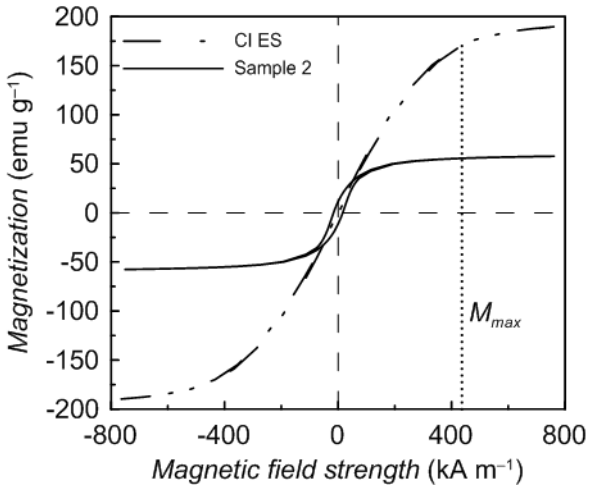

Figure 3. The magnetization curves of CI particles (dashed line) and the Sample 2 particles (solid line). The dotted line represents the magnetization at the highest H_0 used during MR measurements; further referred to as the maximum magnetization M_{max}.

The prepared MR and DMR suspensions exhibit pseudoplastic behavior in the absence of a magnetic field (figure 4), and the DMR suspensions possess a higher viscosity than the MR suspension containing only CI particles. The rod-like particles negatively contribute to the drag forces (friction forces) acting against the direction of the flow. Such systems then display higher viscosity, which can be attributed to the energy needed for the orientation of the particles in the velocity gradient direction [28]. The DMR2–2.5 and DMR2–5 suspensions exhibit higher viscosity than their analogues based on Sample 1. This can be explained as a consequence of the preparation process of the particles that were prepared via thermal decomposition, which led to a higher porosity of the particles connected with an increase in their specific surface area and to a consequent increase in particle-liquid medium interactions, increasing the viscosity of the system.

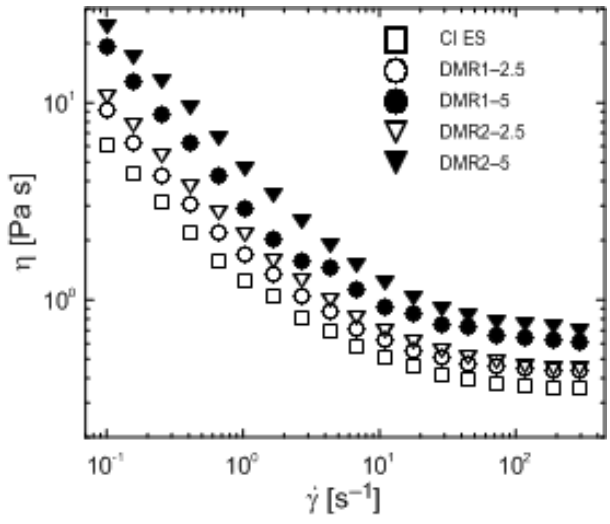

Figure 4. The dependences of shear viscosity, η, on the shear rate, $\dot{\gamma}$, in the absence of a magnetic field for the prepared MR and DMR suspensions.

After the application of a magnetic field, however, the rheological parameters for all prepared suspensions dramatically increase as a consequence of the formation of stiff internal column-like structures following the magnetic field direction. Both DMR suspensions exhibit higher shear stress values than the MR suspensions based on CI particles. The shear stress values of the prepared MR and DMR suspensions increase with the increasing H_0 (figure 5(a-c)). While at the low H_0, the DMR2–2.5 and DMR2–5 suspensions exhibit the highest MR performance (figure 5(a)), with an increasing H_0, both DMR1 suspensions start to exhibit a similar MR effect (figure 5(b), figure 5(c)). At lower magnetic fields ($H_0 << H_{Ms}$; where H_{Ms} represents a magnetic field where the magnetic saturation, M_S, of the particles occurs), magnetic rod-like particles exhibit a more sensitive response than that of the spherical particles due to their magnetic-shape anisotropy [4, 29]. The magnetic rod-like particles orient themselves along with the applied magnetic field, resulting in a higher magnetization and, thus, a larger magnetic moment between the rod-like particles due to shape anisotropy [29, 30]. The MR systems based on rod-like particles therefore exhibit higher MR effects when compared with spherical ones at lower magnetic fields [4, 29].

In the case of the DMR1–2.5 and DMR1–5, the roles of the non-magnetic heterogeneous particles on the enhanced MR performance has been previously described in ref. [23]. In the magnetic field, the columnar structures created from magnetic particles undergo collisions with these non-magnetic particles, leading to stronger viscous dissipation and rotary diffusivity [23]. The collision rate increases with the increasing amount of non-magnetic filler; therefore, the shear stress values are higher for the DMR1–5 than the DMR1–2.5. This explanation clarifies the increased shear stress values for the DMR1–2.5 and the DMR1–5 when compared to MR suspensions based on CI.

With increasing magnetic field intensities (figure 5(c)), the magnetic particles are very close to their M_{max}, and the magnetization is thus significantly higher for CI particles. While at a lower H_0, the τ_y depends on the applied H_0 (Eq. 1 [7]; μ_0 represents vacuum permeability; ϕ is volume fraction of particles).

$$\tau_y = \sqrt{6}\phi\mu_0 {M_S}^{1/2} {H_0}^{3/2} \quad (1)$$

At higher magnetic fields ($H_0 \sim H_{Ms}$), the particles are already fully saturated and their MR performance is independent of the H_0 (Eq. 2 [7]). As a result, the role of the higher M_S of the CI starts to dominate.

$$\tau_y = 0.086\phi\mu_0 {M_S}^2 \quad (2)$$

Thus, at high magnetic fields, the similar MR effects of both DMR based on either magnetic or non-magnetic rods is a consequence of the dominant M_{max} of the CI particles in the suspensions. The prepared magnetic rods possess much lower M_{max} than the CI, which at $H_0 \sim H_{Mmax}$ starts to determine the stiffness of the columnar structures, which adequately explains the observed behavior and fits well with the literature [16]. In figure 5c a certain decrease in shear stress values at low shear rates can be observed for CI ES suspensions. The decrease can be connected with a static (or frictional) yield stress followed by dynamic yielding [6]. This phenomenon was not presented in other samples probably due to their dimorphic nature.

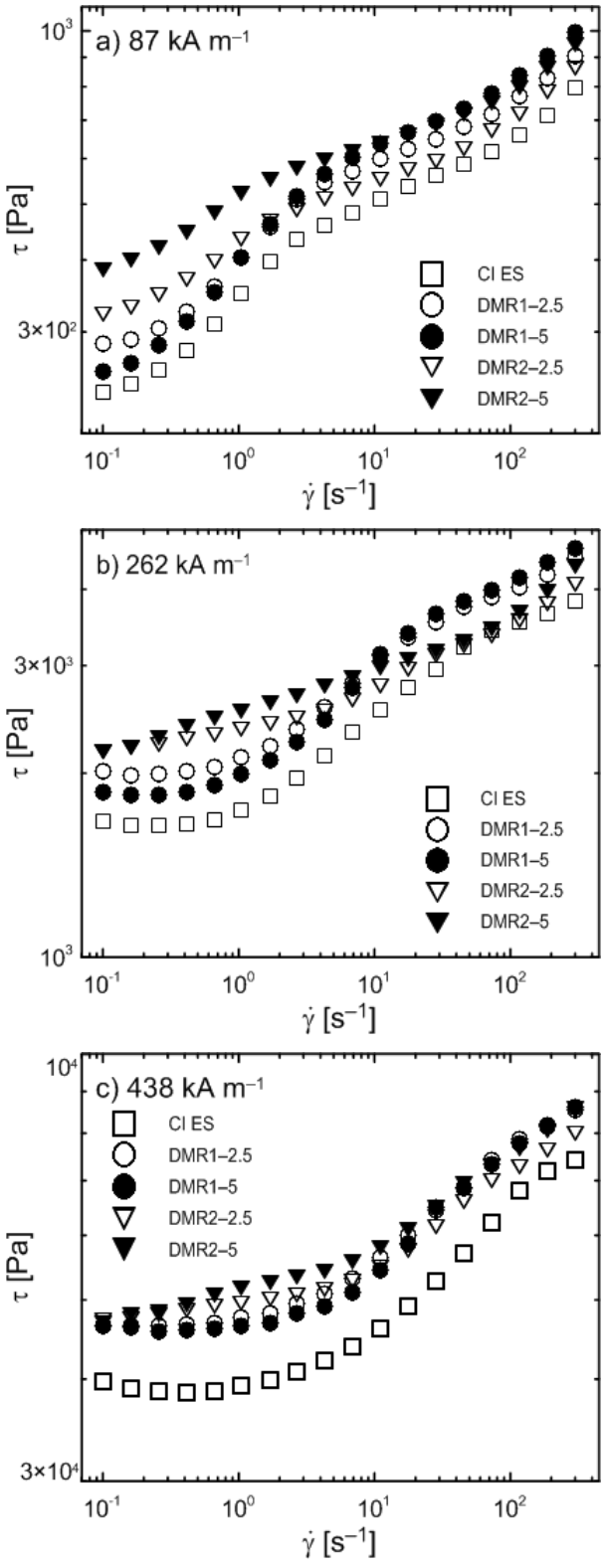

Figure 5. The dependences of shear stress, τ, on the shear rate, $\dot{\gamma}$, for prepared MR and DMR suspensions at (a) 87 kA m^{-1}, (b) 262 kA m^{-1}, and (c) 438 kA m^{-1}.

For the typical MR suspensions, the curves describing the τ vs. $\dot{\gamma}$dependence in magnetic fields $H_0 \sim H_{Ms}$ using double logarithmic dependence (figure 6) measured in controlled shear rate

mode are commonly flat at low shear rates with a small decrease, and further significantly increase when the hydrodynamic forces start to dominate over the magnetic ones. An unusual MR behavior, however, has been observed for DMR2–2.5 and DMR2–5. They do not exhibit any flat region, and their τ values rather increase from very low shear rates. This can be a consequence of magnetic hardening, since the magnetic rod-like particles significantly increase drag force that contributes to an increase of the rheological parameters. In the case of non-magnetic rods, such behavior was not observed since these particles follow the shear force and its velocity vector; thus, only hydrodynamic forces act on them.

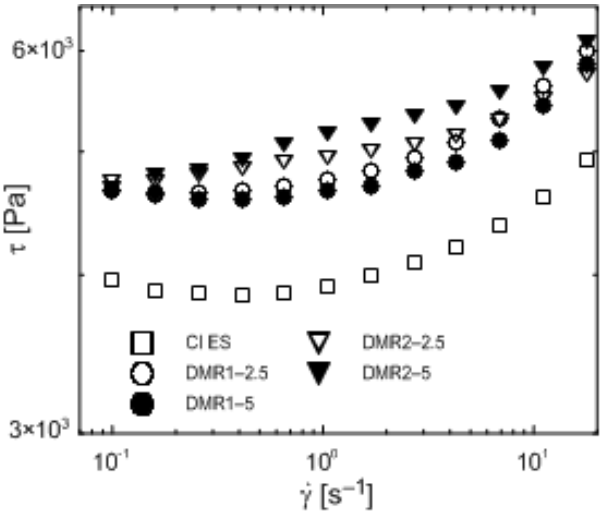

Figure 6. The dependences of shear stress, τ, on the shear rate, $\dot{\gamma}$, for prepared MR and DMR suspensions at 438 kA m^{-1} at low shear rates.

The addition of the rod-like particles into CI-based MR suspensions also positively influenced the sedimentation stability. Both the prepared DMR1 and DMR2 suspensions exhibited higher sedimentation stability than that based on the pure CI particles (figure 7). The relatively-large size of the rod particles thus did not negatively affect the sedimentation stability. Both of the prepared rod-like samples possess lower densities than the used CI, and the shape anisotropy could also positively influence the sedimentation stability when rods can act as a steric barrier. Further, the sedimentation stability of the DMR2 suspension was slightly higher than that of the DMR1 suspension. The particles added into the CI-based MR suspensions make several general positive contributions in slowing down the dispersed particles settling (figure 7): (i) they possess lower densities than the CI particles, causing slower sedimentation and thus a higher stability of the whole system; (ii) they fill the interspace between the particles, preventing them from aggregation, and further, the rod-like particle-CI microsphere agglomerates are formed with an overall density lower than pure CI particles [21]; and (iii),

they increase the height of the stationary phase after the sedimentation process due to lower packing efficiency, which ultimately enhances their redispersibility [21], which was also observed for DMR1 and DMR2. To quantitatively evaluate the influence of rod-like additives to the CI silicone-oil based suspensions on their sedimentation behavior the relaxation times, t_{rel}, were calculated from the obtained data using modified exponential function (Eq. 3)

$$X(t) = X_0 \exp\left(-\frac{t}{t_{rel}}\right)^{\beta} \tag{3}$$

where $X(t)$ and X_0 represent current value of the height of the volume containing the particles in time and the height of the total volume of the suspensions, respectively, t is the real time, and β ($0 < \beta < 1$) accounts for the width of relaxation time distribution; the lower the β value the wider the distribution ($\beta = 1$ for single relaxation time).

Usually the sedimentation process is approximated by a relaxation with single relaxation time which corresponds to $\beta = 1$ [31], however, in the case of heterogeneous systems much better fit (figure 7) was obtained for modified exponential (Eq. 3). In our case extracted values of β were significantly lower for heterogeneous systems (DMR1-5 and DMR2-5) representing wider distribution of relaxation times than for homogeneous CI ES. Also almost doubled relaxation times of heterogeneous systems (table 2), compared to CI ES, reflect the positive contribution of the used rod-like additives on the sedimentation stability of prepared MR suspensions.

Table. 2. Sedimentation parameters of prepared suspensions obtained from Eq. 3.

Parameter	CI ES	DMR1–5	DMR2–5
t_{rel} [h]	7.26	12.82	13.67
β	0.88	0.68	0.69

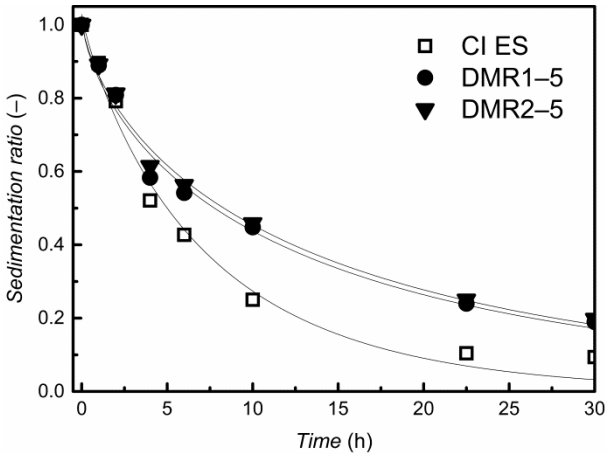

Figure 7. Sedimentation of the diluted MR suspensions. The solid lines represent fits according to Eq. (3). The suspensions were prepared in a concentration of 10 wt%.

Conclusion

The effect of the partial substitution of carbonyl iron particles by either magnetic or non-magnetic rods on the MR behavior of prepared dimorphic magnetorheological suspensions has been investigated. The dimorphic MR suspensions exhibit higher shear stress values than the MR suspensions based on carbonyl iron in the presence of a magnetic field. Distinguishing behavior of prepared MR suspensions was observed at low shear rates. The suspensions based on a mixture of carbonyl iron and magnetic rods exhibited a significant increase in shear stress even at very low shear rates, which could be associated with the effort of magnetic rods to polarize themselves into a direction perpendicular to the shear flow, thus hardening the DMR suspensions. The addition of both types of rod-like particles possessing shape anisotropy as well as lower density compared with carbonyl iron also significantly enhanced the sedimentation stability of the prepared suspensions.

Acknowledgments

This work was supported by the Ministry of Education, Youth and Sports of the Czech Republic – Program NPU I (LO1504).

References

[1] Cvek M, Mrlik M, Ilcikova M, Mosnacek J, Babayan V, Kucekova Z, et al. 2015 The chemical stability and cytotoxicity of carbonyl iron particles grafted with poly(glycidyl methacrylate) and the magnetorheological activity of their suspensions. *RSC Adv* 5(89) 72816-24.

[2] Cvek M, Mrlik M, Ilcikova M, Plachy T, Sedlacik M, Mosnacek J, et al. 2015 A facile controllable coating of carbonyl iron particles with poly(glycidyl methacrylate): a tool for adjusting MR response and stability properties. *J Mater Chem C* 3(18) 4646-56.

[3] Mrlik M, Ilcikova M, Cvek M, Pavlinek V, Zahoranova A, Kronekova Z, et al. 2016 Carbonyl iron coated with a sulfobetaine moiety as a biocompatible system and the magnetorheological performance of its silicone oil suspensions. *RSC Adv* 6(39) 32823-30.
[4] Bell RC, Karli JO, Vavreck AN, Zimmerman DT, Ngatu GT, Wereley NM 2008 Magnetorheology of submicron diameter iron microwires dispersed in silicone oil. *Smart Mater Struct* 17(1) 6.
[5] de Vicente J, Vereda F, Segovia-Gutierrez JP, Morales MD, Hidalgo-Alvarez R 2010 Effect of particle shape in magnetorheology. *J Rheol* 54(6) 1337-62.
[6] de Vicente J, Klingenberg DJ, Hidalgo-Alvarez R 2011 Magnetorheological fluids: a review. *Soft Matter* 7(8) 3701-10.
[7] Ginder JM, Davis LC, Elie LD 1996 Rheology of magnetorheological fluids: Models and measurements. *Int J Mod Phys B* 10(23-24) 3293-303.
[8] Bitaraf M, Ozbulut OE, Hurlebaus S, Barroso L 2010 Application of semi-active control strategies for seismic protection of buildings with MR dampers. *Eng Struct* 32(10) 3040-7.
[9] Zhu XC, Jing XJ, Cheng L 2012 Magnetorheological fluid dampers: A review on structure design and analysis. *J Intell Mater Syst Struct* 23(8) 839-73.
[10] Bucchi F, Forte P, Franceschini A, Frendo F 2013 Analysis of differently sized prototypes of an MR clutch by performance indices. *Smart Mater Struct* 22(10) 10.
[11] Sarkar C, Hirani H 2013 Theoretical and experimental studies on a magnetorheological brake operating under compression plus shear mode. *Smart Mater Struct* 22(11) 12.
[12] Chen ZQ, Wang XY, Ko JM, Ni YQ, Spencer BF, Yang G. MR damping system on Dongting Lake cable-stayed bridge. In: Liu SC, ed. Smart Structures and Materials 2003: Smart Systems and Nondestructive Evaluation for Civil Infrastructures. Bellingham: Spie-Int Soc Optical Engineering 2003, p. 229-35.
[13] Chen ZQ, Wang XY, Ko JM, Ni YQ, Spencer BF, Yang G, et al. 2004 MR damping system for mitigating wind-rain induced vibration on Dongting Lake Cable-Stayed Bridge. *Wind Struct* 7(5) 293-304.
[14] Cvek M, Mrlik M, Pavlinek V 2016 A rheological evaluation of steady shear magnetorheological flow behavior using three-parameter viscoplastic models. *J Rheol* 60 687.
[15] Sedlacik M, Pavlinek V 2014 A tensiometric study of magnetorheological suspensions' stability. *RSC Adv* 4(102) 58377-85.
[16] Bombard AJF, Goncalves FR, Morillas JR, de Vicente J 2014 Magnetorheology of dimorphic magnetorheological fluids based on nanofibers. *Smart Mater Struct* 23(12) 12.
[17] Jiang WQ, Zhang YL, Xuan SH, Guo CY, Gong XL 2011 Dimorphic magnetorheological fluid with improved rheological properties. *J Magn Magn Mater* 323(24) 3246-50.
[18] Ngatu GT, Wereley NM, Karli JO, Bell RC 2008 Dimorphic magnetorheological fluids: exploiting partial substitution of microspheres by nanowires. *Smart Mater Struct* 17(4) 8.
[19] Sedlacik M, Pavlinek V, Vyroubal R, Peer P, Filip P 2013 A dimorphic magnetorheological fluid with improved oxidation and chemical stability under oscillatory shear. *Smart Mater Struct* 22(3) 8.
[20] Ulicny JC, Snavely KS, Golden MA, Klingenberg DJ 2010 Enhancing magnetorheology with nonmagnetizable particles. *Appl Phys Lett* 96(23) 3.
[21] Lopez-Lopez MT, Gomez-Ramirez A, Duran JDG, Gonzalez-Caballero F 2008 Preparation and characterization of iron-based magnetorheological fluids stabilized by addition of organoclay particles. *Langmuir* 24(14) 7076-84.
[22] Machovsky M, Mrlik M, Plachy T, Kuritka I, Pavlinek V, Kozakova Z, et al. 2015 The enhanced magnetorheological performance of carbonyl iron suspensions using magnetic Fe_3O_4/ZHS hybrid composite sheets. *RSC Adv* 5(25) 19213-9.
[23] Rodriguez-Arco L, Lopez-Lopez MT, Kuzhir P, Gonzalez-Caballero F 2014 How nonmagnetic particles intensify rotational diffusion in magnetorheological fluids. *Phys Rev E* 90(1) 11.
[24] Lopez-Lopez MT, de Vicente J, Gonzalez-Caballero F, Duran JDG 2005 Stability of magnetizable colloidal suspensions by addition of oleic acid and silica nanoparticles. *Colloid Surf A-Physicochem Eng Asp* 264(1-3) 75-81.

[25] Rabbani Y, Ashtiani M, Hashemabadi SH 2015 An experimental study on the effects of temperature and magnetic field strength on the magnetorheological fluid stability and MR effect. *Soft Matter* 11(22) 4453-60.
[26] Kozakova Z, Kuritka I, Bazant P, Pastorek M, Babayan V 2015 Magnetic needle-like iron oxide particles prepared by microwave-assisted thermal decomposition technique. *Mater Lett* 138 116-9.
[27] Cao G. Nanostructures & Nanomaterials: Synthesis, Properties & Applications. London: Imperial College Press; 2004.
[28] Vincenzi D 2013 Orientation of non-spherical particles in an axisymmetric random flow. *J Fluid Mech* 719 465-87.
[29] de Vicente J, Segovia-Gutierrez JP, Andablo-Reyes E, Vereda F, Hidalgo-Alvarez R 2009 Dynamic rheology of sphere- and rod-based magnetorheological fluids. *J Chem Phys* 131(19) 10.
[30] Sun L, Hao Y, Chien CL, Searson PC 2005 Tuning the properties of magnetic nanowires. *Ibm J Res Dev* 49(1) 79-102.
[31] Arief I, Mukhopadhyay PK 2014 Preparation of spherical and cubic Fe55Co45 microstructures for studying the role of particle morphology in magnetorheological suspensions. *J Magn Magn Mater* 360 104-8.